scientific reports

Check for updates

OPEN

Behavioral and pathological characteristics of 5xFAD female mice in the early stage

Chenlu Zhu[1,3]✉ & Xuejiao Liu[2,3]

Alzheimer's disease (AD) is a central nervous system degenerative disease with insidious onset and gradual development caused by selective and progressive loss of neurons. The 5xFAD mouse is a relatively mature disease model of AD. However, the behavioral research on 5xFAD female mouse is more focused on the changes of late memory function, and the exploration of its early behavioral and pathological changes is still incomplete. This research aims to explore the changes in memory function, emotional function (including anxiety and depression), motor ability, amyloid plaques, glial cell response and neurogenesis in the hippocampus of female 5xFAD mice in the early stage, laying a foundation for a comprehensive exploration of the disease mechanism of AD. The results of this study found that early 4-month-old female 5xFAD mice mainly showed a decline in memory function without other dysfunction. Accompanied by a large amount of amyloid protein plaques deposited in the hippocampus, it induced the response of microglia and astrocytes, and neurogenesis decreased significantly with age, especially in early female 5xFAD mice, which resulted in a decrease in the number of new neurons. This may be an important reason for the decline in memory function of female 5xFAD mice in the early stage.

Keywords 5xFAD female mice, Early stage, Behavior, Pathological changes

Alzheimer's disease (AD), commonly known as senile dementia, has been a significant focus in the medical field due to its profound impact on patients' lives. As reported by numerous studies[1], AD is characterized by a large number of neuronal loss, beta-amyloid-protein plaque deposition, and Tau protein hyperphosphorylation. These pathological changes manifest as progressive cognitive dysfunction, a decline in memory ability, and can ultimately lead to the loss of basic living abilities and even death[2]. With the continuous intensification of population aging across the globe, as documented by demographic research[3], the prevalence of AD has been steadily rising, imposing an ever-increasing global economic burden[4]. In light of these challenges, clarifying the exact pathogenesis of AD has become a crucial step towards developing effective strategies for delaying its progression and providing appropriate treatment[5].

The exploration of disease mechanisms and the translation of such knowledge into clinical applications rely heavily on the availability of mature and stable disease models. A comprehensive review of the literature[6] reveals that currently, most animal models in AD research are constructed based on genetic factors and pathological changes. Specifically, approaches such as targeted neuronal damage to brain tissue and stereotactic injection of amyloid-protein have been employed, along with the successful construction of some transgenic AD animal models based on gene regulation. The range of animals used in these AD models is quite diverse, including mice, rats, zebrafish, rhesus monkeys, and chimpanzees, most of these models are designed based on only one or more etiological factors of AD onset and consequently fall short in accurately simulating all the complex pathological phenotypes of AD[7]. Hence, within the context of exploring the pathogenesis of AD and identifying potential treatment targets, selecting a suitable animal disease model becomes an extremely critical aspect.

Transgenic 5xFAD mice have emerged as a valuable model in AD research. As demonstrated by prior studies[8,9], these mice can express human FAD mutant APP and PSEN1 genes and possess five AD—related mutation sites, which include three APP-related mutations (Swedish-type (K670N/M671L), Florida-type (I716V), and London-type (V717I) mutations) and two PSEN1-related mutations (M146L and L286V mutations). These mutations work additively to drive excessive production of Aβ42. Moreover, previous research has clearly shown

[1]Department of Neurology, The First Affiliated Hospital of Shandong First Medical University & Shandong Provincial Qianfoshan Hospital, Jinan, China. [2]Department of Hyperbaric Medicine, The First Affiliated Hospital of Shandong First Medical University & Shandong Provincial Qianfoshan Hospital, Jinan, China. [3]Chenlu Zhu and Xuejiao Liu contributed equally to this work. ✉email: zhuchl20@163.com

that 5xFAD mice exhibit intracellular Aβ42 accumulation as early as 1.5 months, followed by amyloid-protein deposition at 2 months, and observable memory loss by 4 months[10].

Neurogenesis, an important aspect in the context of AD, has been the subject of extensive investigation. Multiple studies[11] have established that neurogenesis in AD is an early-onset event and is damaged relatively early, often before the formation of amyloid plaques. For instance, significant damage to neurogenesis can be detected in 2-month-old mice, and by 12 months of age, the loss of layer V pyramidal neurons reaches approximately 40%. Understanding neurogenesis in AD is of particular importance because it may play a crucial role in both the progression of the disease and the identification of potential therapeutic targets. It provides insights into how the brain's regenerative capacity is affected by AD pathology and could potentially guide the development of treatments aimed at restoring or enhancing this regenerative ability.

In addition to the above aspects, sex differences have been observed in AD, both in human patients and in animal models like the 5xFAD mice. As documented by relevant research[12], similar to the onset characteristics of AD patients, the incidence and severity of 5xFAD mice are sex-dependent. Specifically, the incidence and lesion degree of female mice are significantly higher than those of male mice, indicating a strong link between female gender factors and AD. This difference may be attributed to various hormonal and physiological disparities. For example, estrogen, as explored in several studies[13], has been shown to have complex effects on the brain and can potentially influence the progression of AD-related pathologies. Furthermore, it has been noted that the number of neural stem cells in the hippocampal DG of 5xFAD mice is significantly reduced. However, the relationship between this reduction in neural stem cells in AD and possible changes in proliferating stem cells and new neurons, as well as whether it exhibits an age-dependent reduction, remains an area that requires further investigation[14].

Given the unique features of 5xFAD mice in recapitulating multiple aspects of AD pathology and the unresolved questions regarding sex differences and neurogenesis in the context of AD, this study was designed to observe and study the behavioral and pathological characteristics of 5xFAD mice. By doing so, it aims to contribute to a more comprehensive understanding of AD and lay a solid theoretical foundation for subsequent exploration of the mechanisms underlying this complex disease.

Animals

The female 5xFAD mice and C57BL/6J wild-type (WT) mice (20–30 g, 1–4 months old) used in this study were purchased from Beijing VITAL -RIVER Bio-Pharma Technology Co., Ltd., and bred in ShanghaiTech Univercity Model Organisms Center, Inc. All WT mice used in the experiments were littermates of 5xFAD mice. None of the mice used for the experiments had undergone drug testing, and their microbial status was SPF-grade. Mice had free access to sufficient food and water. The indoor temperature was approximately 22 ± 1 ℃, the relative humidity was 60%, and a 12-h day-night cycle was maintained using controlled equipment. There were 2–4 mice per cage. Before the experiment was carried out, all 5xFAD transgenic mice were re-identified for their genotypes by polymerase chain reaction (PCR). All animal experiments obtained the approval of the Institutional Animal Care and Use Committee of Shanghai Tech University. All experiments were performed in strict accordance with the American Veterinary Medical Association (AVMA) Animal Euthanasia Guidelines (2020) and the ARRIVE Guidelines (PLoS Bio 8 (6), e1000412, 2010). This study was approved by the ShanghaiTech University Laboratory Animal Ethics Committee with approval number 20230322001. Throughout the experimental process, we always followed the laboratory animal use and management regulations established by the institution, committed to minimizing animal suffering and ensuring the scientificity and reliability of the experimental data. In this study, the main grouping and the information on the number of mice in each group are as follows: (1) Immunofluorescence staining experiments were conducted using wild-type (WT) mice at the ages of 1, 2, 3, and 4 months and 4-month-old 5xFAD mice. There were a total of 5 groups, with 3 mice in each group. The main immunofluorescence stainings carried out were for Ki67, DCX, GFAP, IBA1 and 6E10. (2) In addition, this study made a comparative analysis of the behavioral experiments of 4-month-old WT mice and 5xFAD mice. There were a total of 2 groups, with 9 mice in each group.

Behavioral experiments

In this study, behavioral experiments on 4-month-old 5xFAD mice were conducted in a stable, quiet, and odor-free environment with fluorescent lights. Feces were pre-cleaned with 75% ethanol between mouse replacements. Experiments were spaced at least 24 h apart. A video camera was installed for behavior capture.

Research reports indicate that the Y-maze, constructed from white opaque polyethylene plastic, comprised three equally long arms. Each arm measured 21 cm in length, 7 cm in width, and 15.5 cm in height, with the branches angled 120 degrees relative to one another[15]. These three branches, labeled A, B, and C, were used in an 8-min behavior detection process. The percentage of spontaneous alternations and the total number of entries into the Y-maze branches were quantified to assess the spatial memory of the mice. The formula for calculating the behavioral evaluation of spontaneous alternations was percentage of spontaneous alternations = (number of alternations) / (total number of arm entries—2) × 100%[16].

The Novel Object Recognition Test (NORT), a method for assessing hippocampus-dependent memory of old objects[17], utilized a plastic rectangular box (50 cm × 35 cm × 15 cm). The experiment had two 5-min stages: training and testing. In the training stage, mice explored two identical spheres. After two hours, one sphere was replaced with a cube, and they explored for 5 min. A camera above the apparatus monitored and recorded the exploration. The time mice interacted with the objects was analyzed and the Discrimination Index (DI), calculated as DI = time of exploring new objects/total exploration time, was used as a cognitive function evaluation standard. Exploratory behavior was defined as any interaction within 2 cm of the object.

The Contextual Fear Conditioning (CFC) experiment assesses animals' learning and memory capabilities, particularly contextual memory reliant on the hippocampus[18]. As per research, the experiment was conducted

in a cylindrical apparatus (18 cm bottom diameter, 30 cm height)[19]. It began with a 2-day environmental familiarization stage. During this period, the mice were placed in a cylindrical apparatus (with a bottom diameter of 18 cm and a height of 30 cm) which constituted the novel environment. This particular environment was devoid of any electrical and sound stimuli, and the mice were allowed to remain therein for 30 min each day, which help the mice to be familiar with the experimental environment. Then, they underwent 3 consecutive days of conditioned-stimulus training, exposed to a 70-decibel sound accompanied by a 0.5 mA, 2-s foot shock 3 times a day, with 20-s rest intervals sans sound and shock. Four days post-shock, the CFC behavior was evaluated using the TSE system (Clever Sys, Inc. Reston, Va, Washington, US). This system automatically recorded the mice's fear-memory behaviors, and memory function was gauged based on the alterations in their movement state before and after the click.

Depression is a typical concomitant of AD. Consequently, this study employed the tail suspension test (TST) and the forced swimming test (FST) to appraise the depression status of 5xFAD mice. For the FST, a cylindrical storage tank crafted from transparent plexiglass, with a height of 30 cm and a bottom diameter of 20 cm, served as the experimental apparatus. Water adjusted to the suitable body temperature (36.5–37.5℃) of mice was introduced into the cylindrical device, and the water level was stabilized at 15 cm from the bottom to preclude the mouse's tail from reaching the tank's floor. In the TST setup, the tail-suspension box measured 55 cm in height, 60 cm in width, and 11.5 cm in depth. The experimental device was constructed from wooden components, and the mouse-suspension apparatus, which consisted of a three-walled rectangular wooden board (55 cm high, 15 cm wide, and 11.5 cm deep), was positioned within this wooden structure. During the mouse-suspension phase, there was no interaction with the surrounding environment. Both tests endured for 6 min, and the depression state of the mice was gauged by the duration for which the mice remained stationary during the experimental period.

The Open-Field Test was primarily employed to assess the anxiety-like behaviors and motor functions of mice[20]. The test apparatus measured 45 cm in width, 45 cm in length, and 50 cm in height, with a central area of 22.5 cm by 22.5 cm. The experiment consisted of two main stages: the adaptation stage and the experimental stage. Initially, the mice were provided with a 2-min adaptation period within the experimental apparatus. Subsequently, they were permitted to freely explore for 10 min. The time spent by the mice in the central area was adopted as an evaluation metric for anxiety-like behavior. The entire experimental process was recorded by the TSE system (TSE, Thuringia, Germany) to facilitate subsequent experimental analysis.

qPCR experiments

According to the manufacturer's protocol, cDNA was extracted from the dentate gyrus (DG) of 5xFAD mouse brain tissue with TRIzol and synthesized using a cDNA Synthesis Kit (Transgene Biotech, Beijing, China, Cat# AT311-03). Quantitative reverse transcription-PCR (qRT-PCR) was carried out with 2 × SYBR Green qPCR Master Mix using a Quant Studio 7 Flex reverse transcription-PCR system (Thermo Fisher Scientific, Cat# 4485700). The reaction conditions were as follows: pre-denaturation at 95°℃ for 20 s, followed by 40 cycles of denaturation at 95°℃ for 15 s, annealing at 60 °C for 30 s, and extension at 72°℃ for 30 s. Primer sequences are shown in Table 1. The relative expression ratio of target gene mRNA was normalized to glyceraldehyde 3-phosphate dehydrogenase (GAPDH) mRNA expression by using the $2^{-\Delta\Delta CT}$ method.

Mouse brain tissue sectioning and immunofluorescence staining experiments

Following fixation of the extracted brain tissues in PFA, gradient dehydration was performed using 20 and 30% sucrose solutions. Brain tissue slices with a thickness of 40 μm were obtained via a vibrating microtome. Tissue slices of the mouse hippocampal DG with similar anatomical structures and positions were selected and washed thrice in PBS for 5 min each. Subsequently, the slices were washed three times in 1 × PBS solution, 5 min per wash. The primary antibody was diluted with antibody diluent (0.3% Triton X-100 + 1% BSA + 1 × PBS) and the tissues were incubated overnight (12–14 h) at 4°℃. After primary antibody incubation, the antibody was recovered the next day and the tissues were washed three times in 1 × PBS for 5 min each. The secondary antibody was diluted with antibody diluent and the brain tissue slices were incubated for 2 h at room temperature. Finally, the nuclei of the brain tissues were stained with DAPI (1 ug/ml, Yeasen, Cat# 40728ES03) solution for 20 min and the mounting of the slices was completed. Throughout the immunofluorescence staining experiment, all

Gene names	Primer sequences
KI67-F	GAGGAGAAACGCCAACCAAGAG
KI67-R	TTTGTCCTCGGTGGCGTTATCC
DCX-F	CTGACTCAGGTAACGACCAAGAC
DCX-R	TTCCAGGGCTTGTGGGTGTAGA
FAD-F	CGGGCCTCTTCGCTATTAC
FAD-I	ACCCCCATGTCAGAGTTCCT
FAD-R	TATACAACCTTGGGGGATGG
GAPDH-F	AGGTCGGTGTGAACGGATTTG
GAPDH-R	TGTAGACCATGTAGTTGAGGTCA

Table 1. Primers used in this study.

Antibody name	Company	Number
6E10	Bio legend	803,004
GFAP	Abcam	ab7260
IBA1	Abcam	ab5076
Ki67	Abcam	Ab16667
DCX	Abcam	ab18723
Goat anti-mouse Alexa Fluor 647	Jackson immuno-research	115-605-003
Goat anti-rabbit Alexa Fluor 555	Thermo fisher scientific	A-21428
Donkey anti-goat Alexa Fluor 555	Thermo fisher scientific	A-21432
Donkey anti-mouse Alexa Fluor 647	Thermo fisher scientific	A-31571

Table 2. Information antibodies used in this study.

operations were carried out in a dark environment to prevent fluorescence quenching due to light exposure. The information of antibodies is summarized in Table 2.

Confocal microscope image acquisition

In this study, a Zeiss LSM980 inverted microscope (Carl Zeiss, Oberkochen, Germany) was employed to randomly acquire confocal images. Fixed voltages and exposure times were set for each fluorescence channel. With the Zeiss LSM 980 confocal microscope, immunofluorescence-stained images of newborn neurons, proliferating cells, amyloid-protein plaques, microglia, and astrocytes were obtained at a tenfold magnification (scale bar = 100 μm). Through manual counting, the numbers of newborn neurons, proliferating cells, amyloid-protein plaques, and glial cells (encompassing microglia and astrocytes) per square millimeter in the mouse hippocampal DG were counted and calculated. Moreover, the tenfold confocal images were processed using ImageJ-win64 software to precisely evaluate the total number of amyloid-protein plaques, the total plaque-covered area, and the average plaque-covered area in the hippocampal DG. The minimum plaque-threshold level was established to guarantee the consistency of all statistical and analytical procedures. The average plaque-area size was determined by dividing the total plaque-covered area by the total number of plaques.

Statistical methods

During the data analysis phase, the blind method was implemented to mitigate potential biases. All measurement data were coded and tallied by an individual who was entirely ignorant of the experimental grouping. In this study, the data of each group were presented as mean ± standard deviation (mean ± SD). GraphPad Prism version 8.0.2 and SPSS Statistics v22 software were utilized for graphing and statistical analysis. Initially, an assessment was made to determine if the data adhered to the normality test. For measurement data that conformed to a normal distribution, the unpaired t-test was employed for comparison between two groups of data. For comparisons among multiple groups of data, a one-way ANOVA single-factor analysis of variance was used and adjusted by the Tukey test method. P value less than 0.05 was indicative of statistical significance.

Results

Decline in memory function of 5xFAD female mice

In order to clarify the behavioral characteristics of 5xFAD mice at 4 months of age, this study designed a variety of experimental methods to detect the memory function and emotional state of the mice. Firstly, the open—field test was used to detect the motor function and anxiety state of 5xFAD mice and WT mice, and it was found that there were no significant differences in the motor ability and anxiety—like state between 5xFAD mice and WT mice (Fig. 1A–C). Then, in order to evaluate the spatial memory ability of the mice, this study carried out the Y—maze experiment (Fig. 1D). Compared with WT mice, the proportion of spontaneous alternation behavior in 5xFAD mice decreased significantly, while the total number of entries into each branch ("arm A, B, C") in the Y—maze device did not change, indicating that the spatial working memory ability of 5xFAD mice decreased while the motor function was normal (Fig. 1E,F). Considering that the spatial working memory ability can be detected and evaluated by a variety of behavioral experiments, in order to ensure the accuracy of memory ability detection, based on the characteristic that mice prefer to explore new objects, this study further selected the novel object recognition test to evaluate the memory function of 5xFAD mice (Fig. 1G). The results of this study showed that the results of the novel object recognition test were consistent with those of the Y—maze experiment. The discrimination ability of 5xFAD mice to new objects decreased significantly, and the memory function was lower than that of WT mice of the same age (Fig. 1H). In addition, this study carried out the contextual fear memory experiment, which mainly included the adaptation stage, the training stage and the test stage (Fig. 1I). During the training stage, the experimental mice were electrically stimulated for three consecutive days to promote the formation of fear memory in the mice, and the fear memory state was evaluated 4 days after the mice were removed from the stimulation conditions. The results of this study showed that before the electrical stimulation, there was no difference in the proportion of time that 5xFAD mice were in a freezing—like behavior state compared with WT mice, while after the electrical stimulation, the proportion of time that 5xFAD mice were in a freezing—like behavior state was significantly lower than that of WT mice, indicating that the fear memory function of 5xFAD mice decreased (Fig. 1J). With the progress of the disease, in addition to the impairment of memory function and the increase in anxiety—like behaviors, AD patients will be accompanied

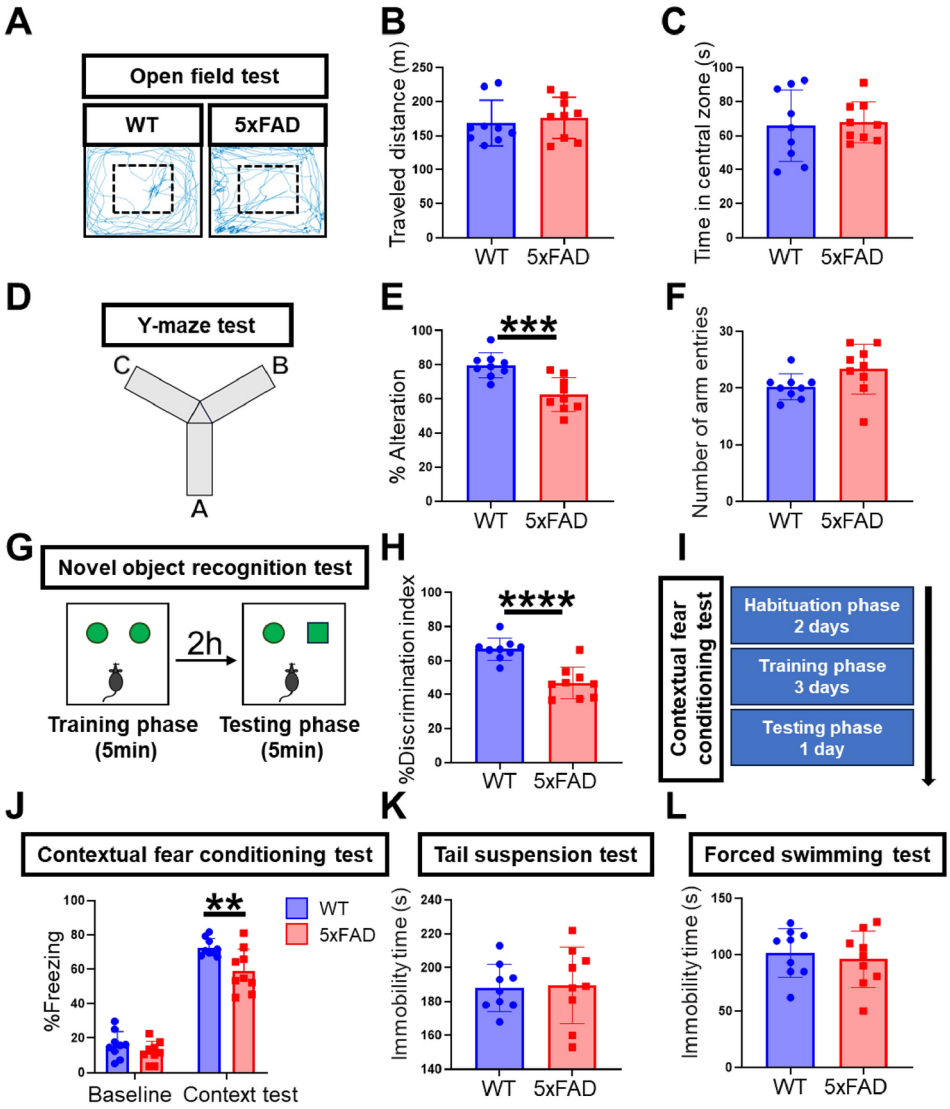

Fig. 1. The memory function of 5xFAD mice declines. (**A**) Trajectory maps of WT mice and 5xFAD mice in the open—field test. (**B**, **C**) There were no statistical differences when comparing the total exploration distance (**B**) and the exploration time in the central area of the experimental device (**C**) between WT mice and 5xFAD mice in the open—field test. n = 9, P > 0.05, vs WT mice. (**D**) Schematic diagram of the Y—maze experiment. (**E**, **F**) In the Y—maze experiment, the probability of correct behavior of 5xFAD mice entering the branches of device arms A, B, and C in sequence was significantly lower than that of WT mice (**E**), while there was no difference in the total number of entries into the device arms between the two types of mice (**F**) n = 9, ***P < 0.001, vs WT mice. (**G**) Schematic diagram of the novel object recognition experiment. (**H**) In the novel object recognition experiment, the discrimination index of 5xFAD mice to new objects was significantly lower than that of WT mice. n = 9, ****P < 0.0001, vs WT mice. (**I**) Schematic diagram of the contextual fear memory experiment, mainly including the adaptation stage, the training stage and the test stage. (**J**) In the test stage of the contextual fear memory experiment, the proportion of time that 5xFAD mice were in a freezing—like state due to fear memory was significantly lower than that of WT mice. n = 9, **P < 0.01, vs WT mice. (**K**, **L**) There were no statistical differences in the behavioral performances of WT mice and 5xFAD mice in the tail suspension test (**K**) and the forced swimming test (**L**). n = 9, P > 0.05, vs WT mice.

by depressive symptoms. In order to clarify whether 4-month-old 5xFAD mice show depressive—like behaviors, this study carried out the forced swimming test and the tail suspension test. Depressive—like behaviors are mainly manifested as an increase in the time that the mice are in a stationary state during the experiment and a decrease in the struggle time. By comparing and analyzing the time that 5xFAD mice and WT mice were in a stationary state in the forced swimming test and the tail suspension test, it was found that there was no statistical difference in the time that the two types of mice were in a stationary state, indicating that 4-month-old 5xFAD mice did not show depressive—like behaviors (Fig. 1K,L). Therefore, 4-month-old 5xFAD mice showed a decline in memory function and no depressive and anxiety—like behavioral manifestations.

Decreased cell proliferation in the hippocampal DG of 5xFAD mice

Neural stem cells undergo cell proliferation and differentiation and gradually form new neurons, and further develop into mature neurons. This phenomenon mainly occurs in the subventricular zone (SVZ) of the lateral ventricle and the subgranular zone (SGZ) of the hippocampal DG. However, neurogenesis gradually declines with age and is severely damaged in neurodegenerative diseases. In order to clarify the age-dependent characteristics of neurogenesis in the hippocampal DG of WT mice and its status in AD diseases, this study detected neurogenesis—related marker molecules, including Ki67, a marker molecule for stem cell proliferation, and DCX, a marker molecule for new neurons. In this study, through the immunofluorescence staining experiment, it was found that the number of Ki67—positive proliferating cells in the hippocampal DG of WT mice showed a gradually decreasing trend with age (Fig. 2A). Compared with 1-month-old WT mice, the number of proliferating cells in the hippocampal DG of 2-month-old, 3-month-old and 4-month-old mice decreased significantly. Moreover, compared with 2-month-old mice, the number of proliferating cells in the hippocampal DG of 3-month-old and 4-month-old mice further decreased and gradually tended to be stable, indicating that the proliferation of neural stem cells shows an age—dependent decreasing characteristic (Fig. 2B). In addition, compared with WT mice of the same age, both the number of Ki67—positive cells and the relative mRNA expression level of Ki67 in the hippocampal DG of 4-month-old 5xFAD mice decreased significantly (Fig. 2C,D).

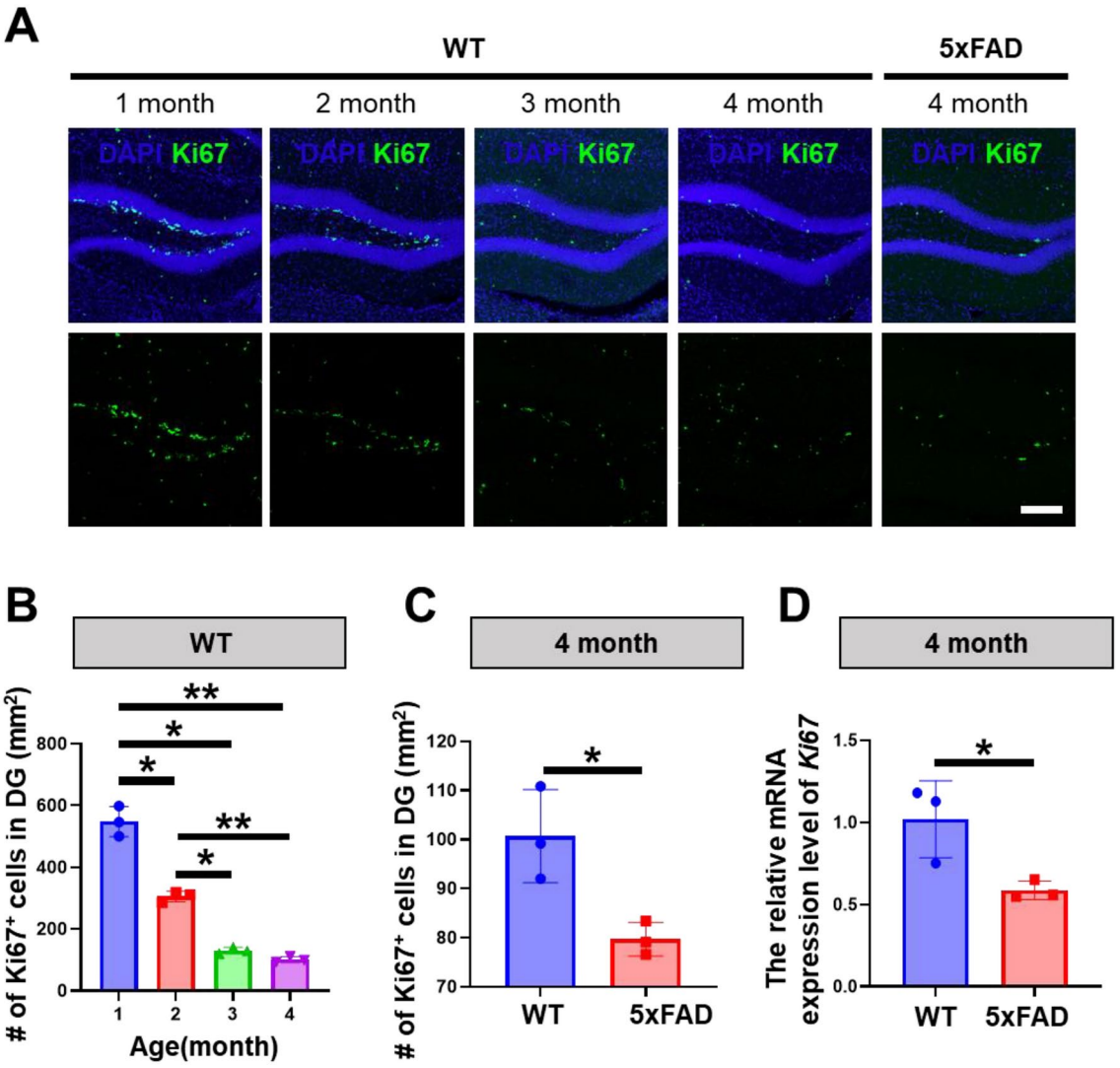

Fig. 2. Cell proliferation in the hippocampal DG decreases as WT mice age, and is significantly decreased in 5xFAD mice of the same age. (**A**) Confocal images of immunofluorescence staining of proliferating cells in the hippocampal DG of 1-to 4-month-old WT mice and 4—month—old 5xFAD mice. Ki67—positive (green, GFP) cells are cells in a proliferating state. Confocal image: magnification is 10—fold, scale bar is 100 μm. (**B**) Count and analyze the number of Ki67—positive (green, GFP) cells in the hippocampal DG of 1-to 4-month-old WT mice, and it is found that the number of proliferating cells gradually decreases with age. n = 3, *P < 0.05, **P < 0.01. (**C**, **D**) Compared with WT mice of the same age, both the number of Ki67—positive proliferating cells (**C**) and the relative mRNA expression level of Ki67 (**D**) in the hippocampal DG of 4-month-old 5xFAD mice are significantly decreased. n = 3, *P < 0.05, vs WT mice.

Decreased neurogenesis in the hippocampal DG of 5xFAD mice

Combined with the above research results, this study believes that the decrease in cell proliferation in the hippocampal DG may be accompanied by impaired neurogenesis, thereby leading to a reduction in the number of new neurons. To verify this conjecture, this study respectively detected the mRNA level of DCX, a marker molecule of new neurons, and the number of DCX-positive new neurons in the hippocampal DG of WT mice and 5xFAD mice. This study found that, compared with WT wild—type mice of the same age, the number of DCX—positive new neurons in the hippocampal DG of 4-month-old 5xFAD mice was significantly reduced (Fig. 3A,B). Moreover, the mRNA expression level of DCX in the hippocampal DG of 4-month-old 5xFAD mice was significantly lower than that of WT mice (Fig. 3C). Therefore, neurogenesis in the hippocampal DG of 4-month-old 5xFAD mice was severely impaired, mainly manifested as a decrease in cell proliferation and the generation of new neurons.

A large number of amyloid—protein plaque depositions and gliosis occurred in the hippocampal DG of 5xFAD mice

Amyloid-protein plaques are one of the common pathological changes in AD and are mainly deposited in the cortex and hippocampal structure. Through the immunofluorescence staining experiment, this study found that a large number of amyloid—protein plaque depositions occurred in the hippocampal DG of 4-month-old 5xFAD mice, while there were almost no amyloid—protein plaque depositions in the hippocampal DG of WT mice of the same age (Fig. 4A,B). The main detection indicators include plaque—covered area (Fig. 4G) and plaque number (Fig. 4H). Moreover, a large number of microglia and astrocytes were aggregated in the hippocampal DG of 5xFAD mice, and these cells were aggregated around the amyloid—protein plaques (Fig. 4A,B). Compared with WT mice, there were more glial cells and a larger covered area in the hippocampal dentate gyrus of 5xFAD mice, mainly including astrocytes (Fig. 4C,D) and microglia (Fig. 4E,F).

The above research indicates that severe amyloid—protein plaque depositions and gliosis occurred in the hippocampal DG of 5xFAD mice. These pathological changes will damage healthy neurons and even inhibit neurogenesis, becoming important reasons for cognitive impairment and memory decline in AD.

Discussion

Under the drive of the Thy1 promoter, mutations occur in the PSEN1 gene and the APP gene, leading to the rapid production of Aβ42 and its rapid accumulation to form amyloid-protein plaques, thereby constructing 5xFAD transgenic mice. 5xFAD mice are an early-stage AD disease model with a relatively fast pathological progression. Their behavioral manifestations are mainly cognitive dysfunction, and declines in memory and learning abilities. Pathological changes mainly include amyloid-protein plaque formation, gliosis, neuroinflammation, neuron loss, synaptic structure destruction, and decreased neurogenesis. These pathological changes are age- and sex-dependent, are interrelated and cross—linked, but not completely synchronous. Research has found that the incidence rate of female AD patients is higher than that of male patients, and pathological changes such as amyloid-protein plaques and neuroinflammation, as well as cognitive dysfunction, are more severe[21,22]. Therefore, this study mainly focuses on the exploration of the behavioral and pathological characteristics of female 5xFAD mice.

Firstly, the abnormal deposition of amyloid-protein plaques, a major pathological hallmark in AD and often utilized for its diagnosis[23], results from an imbalance between Aβ protein production and clearance. APP gene mutations can trigger aberrant gene mRNA generation and function, leading to errors during splicing and translation, which in turn promotes excessive Aβ protein formation. This overwhelms the clearance capacity of glial cells, ultimately resulting in the deposition of various amyloid-protein plaques, namely dense, diffuse, and mixed plaques[24].In the 5xFAD transgenic mice, widely used in AD studies, amyloid-protein aggregation starts at

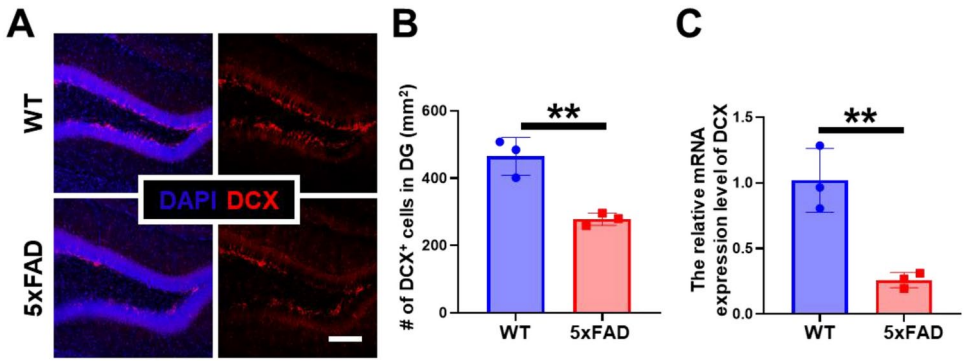

Fig. 3. Decreased neurogenesis in the hippocampal DG of 5xFAD mice. (**A**) Representative confocal images of new neurons (red, DCX) in the hippocampal DG of WT mice and 5xFAD mice. Confocal image: magnification is 10—fold, scale bar is 100 μm. (**B**) Compared with WT mice of the same age, the number of DCX—positive new neurons in the hippocampal DG of 4-month-old 5xFAD mice was significantly decreased. n = 3, **P < 0.01, vs WT mice. (**C**) Compared with WT mice of the same age, the relative mRNA expression level of DCX in the hippocampal DG of 5xFAD mice was significantly decreased. n = 3, **P < 0.01, vs WT mice.

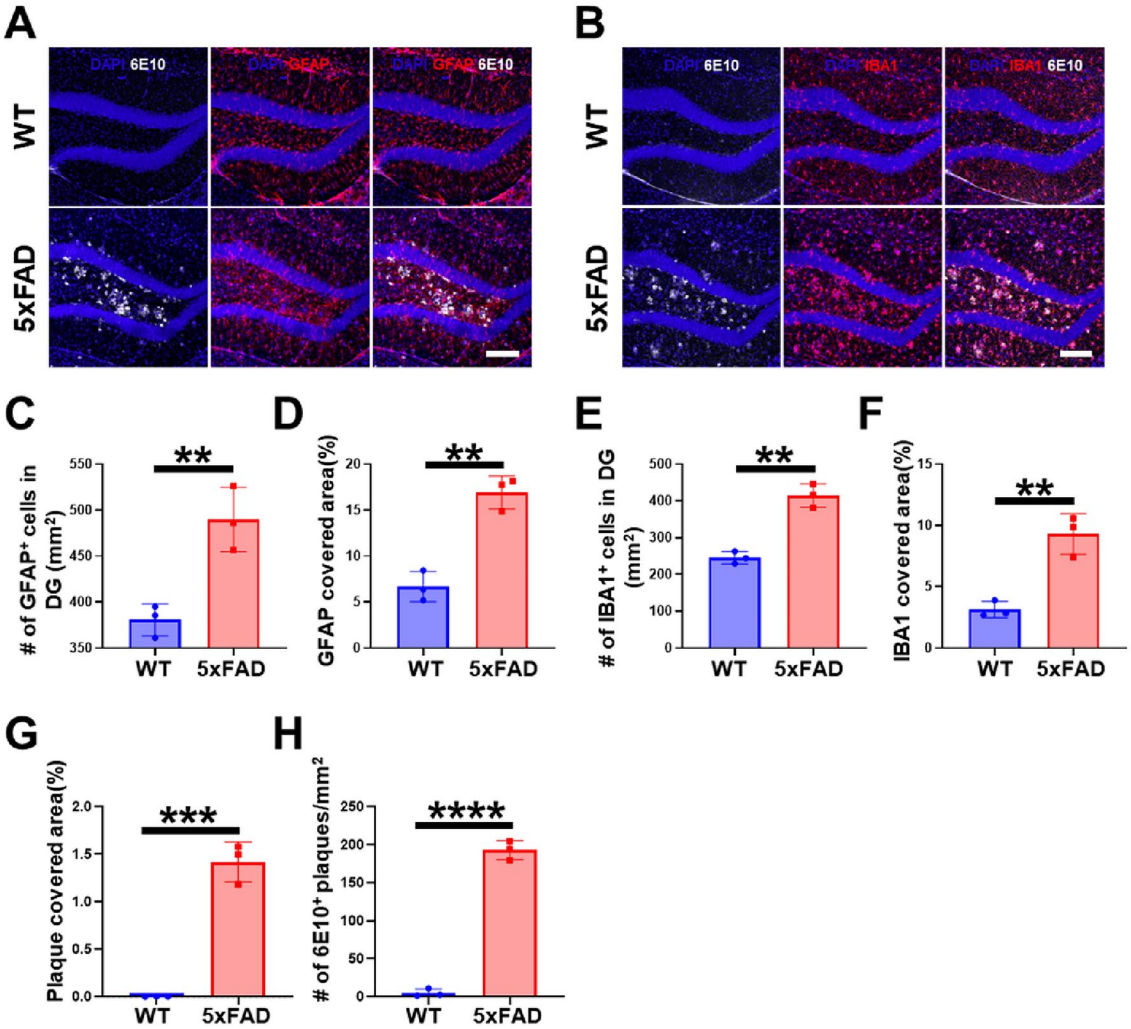

Fig. 4. A large number of amyloid—protein plaque depositions and gliosis occurred in the hippocampal DG of 5xFAD mice. (**A**) Representative confocal images of amyloid—protein plaques (6E10, white) and astrocytes (GFAP, red) in the hippocampal DG of WT mice and 5xFAD mice. Confocal image: magnification is 10—fold, scale bar is 100 μm. (**B**) Representative confocal images of amyloid—protein plaques (6E10, white) and microglia (IBA1, red) in the hippocampal DG of WT mice and 5xFAD mice. Confocal image: magnification is 10—fold, scale bar is 100 μm. (**C**, **D**) Compared with WT mice, there are more astrocytes (**C**) and a larger covered area (**D**) in the hippocampal DG of 5xFAD mice. n = 3, **P < 0.01, vs WT mice. (**E**, **F**) Compared with WT mice, there are more microglia (**E**) and a larger covered area (**F**) in the hippocampal DG of 5xFAD mice. n = 3, **P < 0.01, vs WT mice. (**G**, **H**) For the plaques deposited in the hippocampal DG, the plaque—covered area (**G**) and the total number of plaques (**H**) were mainly analyzed. Compared with WT mice, it was found that severe amyloid—protein plaque depositions occurred in the hippocampal DG of 5xFAD mice. n = 3, ***P < 0.001, ****P < 0.0001, vs WT mice.

1.5 months. Then, as the mice age, plaque formation begins at 2 months and deposits in the hippocampus, cortex, and spinal cord[10]. Of the plaque types, sporadic plaques show stronger neurotoxicity. They, being unrestricted in diffusion and not quickly cleared by glial cells, are prone to harm surrounding neurons and circuits. In contrast, dense plaques, surrounded by glial cells with a tight structure, are less harmful as they have limited access to neurons.

In this study, a large number of amyloid-protein plaques appeared in the hippocampal DG of 4-month-old 5xFAD mice, and a large number of microglia and astrocytes were aggregated around them. Compared with WT mice, the number of glial cells increased significantly. This phenomenon is consistent with previous research reports[25]. The large-scale deposition of amyloid-protein plaques can induce the proliferative response of glial cells, thereby promoting the cascade-like release of inflammatory factors, mainly including IL-1α, IL-1β, IL-6, IL-12, and TNF-α, etc., aggravating nerve damage, and preventing plaque -related glial cell proliferative responses and the generation of neuroinflammation has a significant neuroprotective effect[25]. In fact, in the early stage of the formation of a small number of plaques, glial cells can promote plaque aggregation, prevent their sporadic growth, thereby reducing the risk of plaques destroying healthy neurons, and can promote the

reduction of plaque deposition through phagocytosis. However, once the plaque load is too heavy and exceeds the limit that glial cells can bear, not only can it not be phagocytosed and inhibited by glial cells, but it will also lead to the death and disintegration of glial cells, resulting in the abnormal leakage of a large number of inflammatory factors and the destruction of the structure and function of neurons. Therefore, protecting the normal proliferative response and phagocytic function of glial cells is helpful for reducing neuron damage and maintaining normal neurogenesis, thereby improving the cognitive function in AD.

Traditionally, it is believed that neurogenesis mainly occurs in the embryonic period and early post-natal stage of mammals. After birth, it gradually decreases with age and basically disappears in adulthood. However, since 1960, a large number of studies have shown that there are still continuously proliferating neural stem cells in the adult mammalian brain, mainly concentrated in SVZ and SGZ[26]. However, adult neurogenesis is not static but changes gradually with age. Once neurogenesis is severely damaged, it usually leads to the occurrence of developmental and degenerative diseases. Therefore, exploring ways to enhance neurogenesis and reduce the risk of neurogenesis impairment is very valuable. Previous research reports that increasing physical exercise, enriching the living environment, having a hard diet, and intermittent fasting can stimulate neurogenesis[27–30]. In addition, supplementing mesenchymal stem cells and promoting the proliferation of endogenous neural stem cells can also significantly enhance neurogenesis. However, a decline in sex hormones, chronic stress, abnormal immune function, a high-fat diet, and soft-diet feeding can inhibit neurogenesis, resulting in a reduction in the number of new neurons[31,32]. Therefore, there are multiple risk factors for neurogenesis impairment, and it can also be reversed. In order to explore the state of neurogenesis in the AD hippocampal DG, this study first explored the proliferation of stem cells in the hippocampal DG of WT mice and found that the number of proliferating cells decreased significantly with age, indicating that age is a risk factor for neurogenesis. In addition, this study found that, compared with WT mice of the same age, the cell proliferation and the number of new neurons in the hippocampal DG of 4-month-old 5xFAD mice decreased significantly, and the memory function decreased significantly, indicating that there are severe neurogenesis defects in the hippocampal DG of 5xFAD mice, and this may be one of the important reasons for cognitive dysfunction in AD.

In the context of AD onset, the 4-month-old female 5xFAD mice's early memory decline, along with amyloid plaque and glial cell activation, indicates a possible parallel in human females. Early detection of memory issues and related pathology is thus essential. For progression, the increasing amyloid plaques and decreasing neurogenesis in female 5xFAD mice mirror the worsening in female AD patients. Glial cell response, which may cause chronic inflammation and neuronal damage, is a key factor. Understanding this helps develop strategies to control glial cell activity. Regarding treatment, the identified early changes in female 5xFAD mice offer targets like reducing amyloid plaques or promoting neurogenesis, and modulating glial cell response. Given the link of female hormones to AD, future studies could explore hormonal therapies combined with others. Overall, the female 5xFAD mouse model is valuable for understanding AD in females and creating more specific treatments.

In summary, 5xFAD mice have significant early-stage pathological phenotypes, with significant amyloid-protein plaque deposition and obvious plaque-induced glial cell proliferative responses, while the cell proliferation related to neurogenesis and the generation of new neurons in the AD hippocampal DG are significantly reduced. These changes severely damage the health of neurons and the integrity of neural circuit structures, leading to a significant decline in the memory function of 5xFAD mice. Therefore, 5xFAD mice can be used as an early-stage disease model for studying AD mechanisms.

Conclusion

The number of proliferating cells in the hippocampal DG of WT mice decreases with age, indicating that the proliferation ability of stem cells has the characteristic of age-dependent decline.

The 4-month-old 5xFAD mice have a decline in memory function, and there are impaired neurogenesis, a large number of amyloid-protein plaque depositions and reactive gliosis in their hippocampal DG.

Data availability

Data is provided within the manuscript files. If anyone would like to request data from this study, they should contact Chenlu Zhu at zhuchl20@163.com.

Received: 26 October 2024; Accepted: 12 February 2025
Published online: 26 February 2025

References

1. Oakley, H. et al. Intraneuronal beta-amyloid aggregates, neurodegeneration, and neuron loss in transgenic mice with five familial Alzheimer's disease mutations: potential factors in amyloid plaque formation. *J. Neurosci.* **26**(40), 10129–10140 (2006).
2. Yang, H. et al. Recent progress in nanomedicine for the diagnosis and treatment of Alzheimer's diseases. *ACS Nano* https://doi.org/10.1021/acsnano.4c11966 (2024).
3. Ungvari, A. et al. The role of methionine-rich diet in unhealthy cerebrovascular and brain aging: Mechanisms and implications for cognitive impairment. *Nutrients* **15**(21), 4662 (2023).
4. Singhaarachchi, P. H. et al. Aging, sex, metabolic and life experience factors: Contributions to neuro-inflammaging in Alzheimer's disease research. *Neurosci. Biobehav. Rev.* **162**, 105724 (2024).
5. Yue, C. et al. Atopic dermatitis: pathogenesis and therapeutic intervention. *MedComm* **5**(12), e70029 (2024).
6. De Plano, L. M., Saitta, A., Oddo, S. & Caccamo, A. Navigating Alzheimer's disease mouse models: Age-related pathology and cognitive deficits. *Biomolecules* **14**(11), 1405 (2024).
7. Wang, Q., Zhu, B. T. & Lei, P. Animal models of Alzheimer's disease: Current strategies and new directions. *Zool. Res.* **45**(6), 1385–1407 (2024).
8. Pádua, M. S., Guil-Guerrero, J. L. & Lopes, P. A. Behaviour hallmarks in Alzheimer's disease 5xFAD mouse model. *Int. J. Mol. Sci.* **25**(12), 6766 (2024).

9. Kourti, M. & Metaxas, A. A systematic review and meta-analysis of tau phosphorylation in mouse models of familial Alzheimer's disease. *Neurobiol. Dis.* **192**, 106427 (2024).
10. Demars, M. et al. Impaired neurogenesis is an early event in the etiology of familial Alzheimer's disease in transgenic mice. *J. Neurosci. Res.* **88**(10), 2103–2117 (2010).
11. la Barbera, L. & D'Amelio, M. Alzheimer's disease and sex-dependent alterations in the striatum: A lesson from a mouse model. *J. Alzheimers Dis.* **94**(4), 1377–1380 (2023).
12. Bayer, T. A. & Wirths, O. Intraneuronal Aβ as a trigger for neuron loss: can this be translated into human pathology?. *Biochem. Soc. Trans.* **39**(4), 857–861 (2011).
13. Suganya, S., Ashok, B. S. & Ajith, T. A. A recent update on the role of estrogen and progesterone in Alzheimer's disease. *Cell Biochem. Funct.* **42**(8), e70025 (2024).
14. Marei, H. E., Khan, M. U. A. & Hasan, A. Potential use of iPSCs for disease modeling, drug screening, and cell-based therapy for Alzheimer's disease. *Cell Mol. Biol. Lett.* **28**(1), 98 (2023).
15. Kraeuter, A. K., Guest, P. C. & Sarnyai, Z. The Y-maze for assessment of spatial working and reference memory in mice. *Methods Mol. Biol.* **1916**, 105–111 (2019).
16. Kang, S. et al. Effects of a dehydroevodiamine-derivative on synaptic destabilization and memory impairment in the 5xFAD, Alzheimer's disease mouse model. *Front. Behav. Neurosci.* **12**, 273 (2018).
17. Lueptow, L. M. Novel object recognition test for the investigation of learning and memory in mice. *J. Vis. Exp.* https://doi.org/10.3791/55718-v (2017).
18. Danielson, N. B. et al. Distinct contribution of adult-born hippocampal granule cells to context encoding. *Neuron* **90**(1), 101–112 (2016).
19. Kimura, R. & Ohno, M. Impairments in remote memory stabilization precede hippocampal synaptic and cognitive failures in 5XFAD Alzheimer mouse model. *Neurobiol. Dis.* **33**(2), 229–235 (2009).
20. Seibenhener, M. L. & Wooten, M. C. Use of the open field maze to measure locomotor and anxiety-like behavior in mice. *J. Vis. Exp.* **96**, e52434 (2015).
21. Poon, C. H. et al. Sex differences between neuronal loss and the early onset of amyloid deposits and behavioral consequences in 5xFAD transgenic mouse as a model for Alzheimer's disease. *Cells* **12**(5), 780 (2023).
22. Sil, A. et al. Sex differences in behavior and molecular pathology in the 5XFAD model. *J. Alzheimers Dis.* **85**(2), 755–778 (2022).
23. Kim, K. et al. Anti-amyloidogenic indolizino[3,2-c]quinolines as imaging probes differentiating dense-core, diffuse, and coronal plaques of amyloid-β. *RSC Med. Chem.* **12**(11), 1926–1934 (2021).
24. Ma, C., Hong, F. & Yang, S. Amyloidosis in Alzheimer's disease: Pathogeny, etiology, and related therapeutic directions. *Molecules* **27**(4), 1210 (2022).
25. Lindsay, A., Hickman, D. & Srinivasan, M. A nuclear factor-kappa B inhibiting peptide suppresses innate immune receptors and gliosis in a transgenic mouse model of Alzheimer's disease. *Biomed. Pharmacother.* **138**, 111405 (2021).
26. Boldrini, M. et al. Human hippocampal neurogenesis persists throughout aging. *Cell Stem Cell* **22**(4), 589–99.e5 (2018).
27. Grońska-Pęski, M., Gonçalves, J. T. & Hébert, J. M. Enriched environment promotes adult hippocampal neurogenesis through FGFRs. *J. Neurosci.* **41**(13), 2899–2910 (2021).
28. Ben-Zeev, T., Shoenfeld, Y. & Hoffman, J. R. The effect of exercise on neurogenesis in the brain. *Isr Med. Assoc. J.* **24**(8), 533–538 (2022).
29. Utsugi, C. et al. Hard-diet feeding recovers neurogenesis in the subventricular zone and olfactory functions of mice impaired by soft-diet feeding. *PLoS ONE* **9**(5), e97309 (2014).
30. Baik, S. H. et al. Intermittent fasting increases adult hippocampal neurogenesis. *Brain Behav.* **10**(1), e01444 (2020).
31. Yao, X. et al. High-fat diet consumption in adolescence induces emotional behavior alterations and hippocampal neurogenesis deficits accompanied by excessive microglial activation. *Int. J. Mol. Sci.* **23**(15), 8316 (2022).
32. Yamamoto, T. et al. Soft-diet feeding inhibits adult neurogenesis in hippocampus of mice. *Bull. Tokyo Dent. Coll.* **50**(3), 117–124 (2009).

Acknowledgements

We are grateful for the support provided by ShanghaiTech University. The First Affiliated Hospital of Shandong First Medical University provided excellent administrative support. Finally, we thank the reviewers and editors for their insightful comments and suggestions.

Author contributions

Zhu Chenlu completed the design, operation and data analysis of all experiments, and wrote the manuscript. Liu Xuejiao participated in the revision of the manuscript, and all authors agreed to the publication of the study.

Declarations

Competing interests

The authors declare no competing interests.

Ethics approval

The approval number is 20230322001, and the approval date is March 22, 2023.

Consent for publication

All authors have reviewed and agreed to publish this paper.

Additional information

Supplementary Information The online version contains supplementary material available at https://doi.org/10.1038/s41598-025-90335-2.

Correspondence and requests for materials should be addressed to C.Z.

Reprints and permissions information is available at www.nature.com/reprints.

Publisher's note Springer Nature remains neutral with regard to jurisdictional claims in published maps and institutional affiliations.